



**HAL**  
open science

## Transferability of continuous- and class-pedotransfer functions to predict water retention properties of semiarid Syrian soils

Hassan Al Majou, B Hassani, Ary Bruand

► **To cite this version:**

Hassan Al Majou, B Hassani, Ary Bruand. Transferability of continuous- and class-pedotransfer functions to predict water retention properties of semiarid Syrian soils. *Soil Use and Management*, 2018, 34, pp.354-369. 10.1111/sum.12424 . insu-01857103

**HAL Id: insu-01857103**

**<https://insu.hal.science/insu-01857103v1>**

Submitted on 14 Aug 2018

**HAL** is a multi-disciplinary open access archive for the deposit and dissemination of scientific research documents, whether they are published or not. The documents may come from teaching and research institutions in France or abroad, or from public or private research centers.

L'archive ouverte pluridisciplinaire **HAL**, est destinée au dépôt et à la diffusion de documents scientifiques de niveau recherche, publiés ou non, émanant des établissements d'enseignement et de recherche français ou étrangers, des laboratoires publics ou privés.

1 **Transferability of continuous- and class-pedotransfer functions to predict water**  
2 **retention properties of semiarid Syrian soils**

3

4

5 H. Al Majou<sup>a b\*</sup>, B. Hassani<sup>c</sup>, A. Bruand<sup>a</sup>

6

7 *<sup>a</sup>Institut des Sciences de la Terre d'Orléans (ISTO), Université d'Orléans, CNRS/INSU,*  
8 *BRGM, 1A Rue de la Férollerie, 45071 Orléans Cedex 2, France.*

9 *<sup>b</sup>Department of Soil Science, Faculty of Agronomy, University of Damascus, PO Box*  
10 *30621, Damascus, Syria.*

11 *<sup>c</sup>Department of Soil & Land Reclamation, Faculty of Agriculture, Aleppo University, Aleppo,*  
12 *Syria.*

13

14 **\*Corresponding author:** email Hassan.Almajou@univ-orleans.fr

15

16 **Running title:** Water retention properties of semiarid Syrian soil

17

## 18 **Abstract**

19 Hydraulic properties of soils, particularly water retention, are key for appropriate management  
20 of semiarid soils. Very few pedotransfer functions (PTFs) have been developed to predict  
21 these properties for soils of Mediterranean regions, where data are particularly scarce. We  
22 investigated the transferability of PTFs to semiarid soils. The quality of the prediction was  
23 compared to that for soils originating from temperate regions for which most PTFs were  
24 developed. We used two soil datasets, one from the Paris basin (French dataset,  $n = 30$ ), and a  
25 Syrian dataset ( $n = 30$ ). Soil samples were collected in winter when the water content was  
26 near field capacity. Composition and water content of the samples were determined at seven  
27 water potentials. Continuous- and class-PTFs developed using different predictors were tested  
28 using the two datasets and their performance compared to those developed using artificial  
29 neural networks (ANN). The best performance and transferability of the PTFs for both  
30 datasets used soil water content at field capacity as predictor after stratification by texture.  
31 The quality of prediction was similar to that for ANN-PTFs. Continuous- and class-PTFs may  
32 be transferable to other countries with performances that vary according to their ability to  
33 account for variation in soil composition and structure. Taking into account predictors of  
34 composition (particle size distribution, texture, organic carbon content) and structure (bulk  
35 density, porosity, field capacity) did not lead to a better performance and best transferability  
36 potential.

37 **Keywords:** Pedotransfer functions, Soil water retention, Syrian soils, Field capacity, Texture,  
38 Bulk density.

39

## 40 **Introduction**

41 The hydraulic properties of soils, particularly soil water retention properties, are key data for  
42 the appropriate management of soils. These properties, which are generally unavailable and

43 expensive to measure, can be predicted from other more easily measured properties using  
44 prediction tools called “pedotransfer functions (PTFs)” (Bouma, 1989). PTFs have been  
45 applied in a large number of studies in recent decades (e.g. Cornelis *et al.*, 2001; Wösten *et*  
46 *al.*, 2001; Al Majou *et al.*, 2007; Nasta *et al.*, 2009; Haghverdi *et al.*, 2015; Nemes, 2015;  
47 Khlosi *et al.*, 2016; Nguyen *et al.*, 2017).

48 PTFs can be grouped into two categories, continuous-PTFs and class-PTFs (Wösten *et al.*,  
49 1999). Continuous-PTFs enable the continuous prediction of the water retention curve (WRC)  
50 over the whole soil water content range, i.e. from water saturation to residual water content  
51 (e.g. Vereecken *et al.*, 1989; Wösten *et al.*, 1999; Hodnett & Tomasella, 2002; Al Majou *et*  
52 *al.*, 2008a; Ghorbani *et al.*, 2010; Haghverdi *et al.*, 2012; Medrado & Lima, 2014) (Table 1).  
53 The class-PTFs predict the water retention curve discontinuously by grouping the data  
54 according to the functional behaviour of different horizons but may also be grouped according  
55 to some other criteria, such as texture or bulk density (Wösten *et al.*, 1990; Baker, 2008).  
56 Thus, a single mean value or several mean values of the hydraulic properties are selected to  
57 represent each class (Wösten *et al.*, 1999; Schaap *et al.*, 2001; Hodnett & Tomasella, 2002;  
58 Nemes, 2002; Bruand *et al.*, 2003; Pachepsky *et al.*, 2006; Al Majou *et al.*, 2007). Class-PTFs  
59 are often easy to use because they usually require little information about the soil compared  
60 with most continuous-PTFs that are more demanding of soil characteristics (Lilly *et al.*, 1999;  
61 Nemes *et al.*, 2003). However, they are often regarded as leading to poorer quality predictions  
62 than continuous-PTFs (Wösten *et al.*, 1995). The issue of whether WRC prediction is best  
63 carried out with continuous-PTFs or with class-PTFs is still debated (Wösten *et al.*, 1999;  
64 Medeiros *et al.*, 2014) as is the issue of their transferability to other regions than those from  
65 which the soils originated to establish the PTFs considered (Cresswell *et al.*, 2006; Touil *et*  
66 *al.*, 2016). Few studies relate to the prediction of the WRC of soils in the Mediterranean basin  
67 (Dridi & Dilmi, 2011; Mohawesh, 2013; Wösten *et al.*, 2013). Thus, in Syria and in other

68 countries of the Mediterranean basin, there is still little information available on hydraulic  
69 properties of soils and establishment of national soil databases is only just beginning  
70 (Sommer *et al.*, 2012; Khlosi *et al.*, 2013).

71 Other approaches, such as artificial neural networks (ANN) (Haykin, 1994; Schaap *et al.*,  
72 2001), support vector machines (SVM) (Twarakavi *et al.*, 2009) or the k-nearest neighbor  
73 technique (k-NN) (Nemes *et al.*, 2006a) have also been developed in recent decades to predict  
74 the water retention properties of soils. The approach using artificial neural networks (ANN)  
75 use one or more hidden layers or hidden units and are based on a self-learning process by  
76 using a set of soils for which the water retention properties and the basic properties are known  
77 (Table 1). Artificial neural network-based PTFs were introduced by Pachepsky *et al.* (1996)  
78 and Schaap and Bouten (1996). Unlike continuous- and class-PTFs, they do not require an a  
79 priori model (e.g. linear or exponential functions) (Nemes *et al.*, 2002). During the last two  
80 decades, ANNs have been used extensively to predict soil water retention and their  
81 performance has been compared with PTFs based on other approaches (Minasny *et al.*, 2004;  
82 Twarakavi *et al.*, 2009; Nguyen *et al.*, 2017).

83 The objective of the present study was to select continuous- and class-PTFs from the literature  
84 and to analyze the quality of prediction when used for a set of French soils and a set of Syrian  
85 soils originating from temperate and Mediterranean regions, respectively. Prediction  
86 performance results for the selected continuous- and class-PTFs were also compared with  
87 those for ANN-PTFs. Additionally, their transferability to soil in France and Syria were  
88 assessed, given that the compared PTFs were established with soil samples from different  
89 origins.

90

## 91 **Materials and methods**

### 92 *Soil data sets*

93 A first set of soil samples was collected in France. Thus, 30 horizons (12 horizons A or Ap  
94 and 18 horizons E, B or C) originating from soils developed on sedimentary rocks in the Paris  
95 basin were sampled in winter. The climate of the Paris basin is temperate and influenced by  
96 the Atlantic Ocean, according to the distance from the coast. The soils were Cambisols,  
97 Luvisols and Fluvisols (ISSS Working Group R.B., 1998) (Bruand & Tessier, 2000).

98 Another set of soil samples was collected in Syria. The soil samples were also collected in  
99 winter between latitudes 32 and 37° N and longitudes 35 to 42° E, an area with a  
100 Mediterranean or degraded Mediterranean climate (Rigot, 2006). Along the coast, the climate  
101 is Mediterranean but continental influences and aridity contribute to a rapid degradation of the  
102 Mediterranean climate as the distance from the coast increases. A set of 30 horizons (16  
103 horizons A or Ap and 14 horizons E, B or C) resulting from four sites were chosen as being  
104 representative of the main soil types. They were developed on calcareous and volcano-  
105 sedimentary (basaltic) parent materials and collected in Aridisols, Inceptisols and Vertisols  
106 (Ilaiwi, 1980; Yuksel, 1982; Land Classification and Soil Survey of the Syrian Arab Republic,  
107 1982) or Calcisols, Gypsisols, Inceptisols and Vertisols (van Liere, 1995).

108 For each horizon, the particle size distribution without decarbonation (Robert & Tessier,  
109 1974), the bulk density of clods and horizons (Bruand & Tessier, 2000), the organic carbon  
110 content by oxidation using an excess amount of potassium dichromate in a sulphuric acid  
111 controlled at 135°C (Baize, 2000), the CaCO<sub>3</sub> content (Dupuis, 1969) and cation exchange  
112 capacity (CEC) (Ciesielski & Sterckeman, 1997) were determined. The volumetric water  
113 content was determined for the 60 soil samples from the two datasets at the water potential  
114 values -10 hPa ( $\theta_{1,0}$ ), -33 hPa ( $\theta_{1,5}$ ), -100 hPa ( $\theta_{2,0}$ ), -330 hPa ( $\theta_{2,5}$ ), -1000 hPa ( $\theta_{3,0}$ ), -3300  
115 hPa ( $\theta_{3,5}$ ), -15000 hPa ( $\theta_{4,2}$ ) using the pressure plate extractor method (Bruand & Tessier,  
116 2000).

117 ***The continuous- and class-PTFs selected***

118 Among continuous-PTFs, some enable the direct prediction of the parameters of a WRC  
119 model (Table 1). In most studies, these continuous-PTFs are multiple linear regressions or  
120 non linear regressions providing the parameters of the van Genuchten model (1980) as output  
121 variables by using the particle size distribution, the organic carbon content and the bulk  
122 density as input soil properties (e.g. Tomasella *et al.*, 2003; Schaap *et al.*, 2001) (Fig. 1a).  
123 Among this group of continuous-PTFs, those established with a large number of European  
124 soils (Wösten-continuous-PTFs, see Table 5 in Wösten *et al.* 1999), with Belgian soils  
125 (Vereecken-continuous-PTFs, see Table 7 in Vereecken *et al.*, 1989), and with French soils  
126 (VG-continuous-PTFs, see Table 6 in Al Majou *et al.*, 2008a) were selected for this study  
127 (Table 1). They all estimate the parameters of the van Genuchten model (1980).

128 Other continuous-PTFs do not directly predict the parameters of a WRC model but rather the  
129 water content at several matric potentials as output variables, generally by using the particle  
130 size distribution, the organic carbon content and the bulk density as input data (e.g. Pachepsky  
131 & Rawls, 1999; Reichert *et al.*, 2009; Ghanbarian & Millán, 2010; Minasny & Hartemink,  
132 2011) (Fig. 1b). Then, knowing the water content at different water potentials, a WRC model  
133 is adjusted to the predicted water contents. Among this group of continuous-PTFs, those  
134 established with Brazilian soils (Reichert-continuous-PTFs, see Table 4 in Reichert *et al.*,  
135 2009), with French soils (PSD-continuous-PTFs and FC-continuous-PTFs, see Table 4 & 5 in  
136 Al Majou *et al.*, 2008a), with soils originating from the USA (Ghanbarian-continuous-PTFs,  
137 see Table 5 model 1 in Ghanbarian & Millán, 2010) and with soils originating from tropical  
138 regions (Minasny-continuous-PTFs, see section 5.1 in Minasny & Hartemink., 2011) were  
139 selected for this study (Table 1). They estimate water contents at three to seven values of  
140 water potential and concern a large range of soil types.

141 On the other hand, some of the class-PTFs directly predict the parameters of a WRC model  
142 after stratification according to soil characteristics such as texture, bulk density, the type of

143 horizon or type of soil, as input data (Table 1, Fig. 1c). Among this group of class-PTFs, those  
144 established after stratification by texture alone, and by both the type of horizon and texture  
145 with soils originating from North America (Schaap-class-PTFs, see Table 1 in Schaap *et al.*,  
146 2001), Europe (Wösten-class-PTFs, see Table 4 in Wösten *et al.*, 1999) and France (T-H-VG-  
147 class-PTFs, see Table 3 in Al Majou *et al.*, 2008a), respectively, were selected for this study  
148 (Table 1).

149 Finally, other class-PTFs are sets of water contents at different values of water potential, these  
150 water contents being related also to classes of soil characteristics such as texture, bulk density,  
151 the type of horizon or type of soil, as input data (Table 1, Fig. 1d). Among this group of class-  
152 PTFs, those established with French soils after stratification by either texture alone, by both  
153 texture and bulk density or by all the three predictors texture, bulk density and type of horizon  
154 (T-FC-class-PTFs, see Tables 5 Al Majou *et al.*, 2008a; T-class-PTFs, T-BD-class-PTFs, T-  
155 BD-H-class-PTFs, see Tables 2, 4 and 5 in Al Majou *et al.*, 2008b) and providing sets of  
156 water content at seven values of water potential were selected for this study.

### 157 ***The Artificial Neural Networks-PTFs***

158 The type of ANN selected was the one most commonly used to predict the hydraulic  
159 properties of soils (Børgesen & Schaap, 2005; Fashi, 2014). It usually consists of a three-layer  
160 feed forward back propagation network using, for each model, input layers (basic soil  
161 properties), hidden layers, and output layers (soil hydraulic properties), (Fig. 1e). Each neuron  
162 of the hidden layer calculates the sum  $s$ , of a weighted combination  $w_i$ , of its input signals  $x_i$ ,  
163 and a bias term  $w_0$ , and passes the result through the activation functions that were tangent  
164 hyperbolic and linear in the hidden and output layers, respectively.

$$165 \quad s = \sum_{i=1}^n w_i x_i + w_0 \quad (1)$$



166 The Levenberg-Marquardt algorithm (Demuth & Beale, 2000) was implemented to speed up  
 167 the training of the multi-layer feed-forward neural network. The number of neurons in the  
 168 hidden layer has to be found through trial and error; the number tested here varied from 1 to  
 169 10 neurons. The feed-forward process stops once the output is predicted. Back-propagation  
 170 algorithms try to minimize the error (minimize the sum of squares of the residuals between  
 171 the measured and predicted outputs) of the mathematical system represented by the neural  
 172 network's weights. The error is estimated as the difference between the actual and computed  
 173 outputs.

174 The French national database used by Al Majou *et al.* (2008b) to develop continuous- and  
 175 class-PTFs, including those discussed in this study, and which consists of 456 samples was  
 176 used to train and evaluate the predictive performance of the ANN developed (Table 2). To  
 177 continue to test the ANN method, the ANN developed was then applied to the French and  
 178 Syrian datasets. The ANN simulations were performed by using the neural network toolbox  
 179 provided by Matlab (R2014b).

180 ***Criteria used to evaluate the performance of the continuous- and class-PTFs***

181 To assess the continuous and class-PTFs performance, we used the mean error of prediction  
 182 (MEP) and the standard deviation of prediction (SDP) which provide information on the  
 183 estimation bias and precision, respectively, as follows:

184 
$$MEP = \frac{1}{l' \cdot l} \sum_{j=1}^{l'} \sum_{i=1}^l (\theta_{p,j,i} - \theta_{m,j,i}) \quad (2)$$

185 
$$SDP = \left\{ \frac{1}{l' \cdot l} \sum_{j=1}^{l'} \sum_{i=1}^l [(\theta_{p,j,i} - \theta_{m,j,i}) - MEP]^2 \right\}^{1/2} \quad (3)$$

186

187 where  $\theta_{p,j,i}$  is the predicted water content at matric potential  $i$  for the horizon  $j$ ,  $\theta_{m,i,j}$  is the  
 188 measured water content at matric potential  $i$  for the horizon  $j$ , and  $l$  is the number of matric  
 189 potentials for each horizon ( $l=7$  in this study) and  $l'$  is the number of horizons studied.

190 The root mean square error (*RMSE*) which is commonly used to test PTFs (e.g. Wösten *et al.*,  
 191 2001; Schaap, 2004; Lamorski *et al.*, 2008) and which varies according to both the overall  
 192 prediction bias and the overall prediction precision was also computed:

193

$$194 \quad RMSE = \left\{ \frac{1}{l' \cdot l} \sum_{j=1}^{l'} \sum_{i=1}^l (\theta_{p,j,i} - \theta_{m,j,i})^2 \right\}^{1/2} \quad (4)$$

195 Beside these three statistical criteria, the coefficient of determination ( $R^2$ ) was computed:

$$196 \quad R^2 = 1 - \frac{\sum_{j=1}^{l'} \sum_{i=1}^l (\theta_{p,j,i} - \theta_{m,j,i})^2}{\sum_{j=1}^{l'} \sum_{i=1}^l (\theta_{m,j,i} - \bar{\theta}_{m,i})^2} \quad (5)$$

197 where  $\bar{\theta}_{m,i}$  represents the average of the measured water content at the matric potential  $i$ . The  
 198 value of the coefficient of determination ( $R^2$ ) measures the strength of the linear relation  
 199 between the predicted and measured values.

## 200 **Results and discussion**

### 201 ***Characteristics of the studied soils***

202 The studied horizons showed Fine, Very Fine or Medium texture in the European triangle of  
 203 texture (Commission of the European Communities, 1985) and no coarse elements (Table 2,  
 204 Fig. 2a). Particle size distribution mean values for the datasets from France and Syria were  
 205 close (Fig. 2b–c). However, the Syrian dataset showed a smaller mean OC content because of  
 206 the higher temperatures, limited precipitation and tillage systems that rapidly oxidize organic  
 207 matter (Mrabet, 2011). As for the smaller mean bulk density of the Syrian soils, it can be

208 attributed to a larger macroporosity in most horizons as observed in the field (data not  
209 shown). The mean  $\text{CaCO}_3$  content and CEC were greater in the Syrian dataset.

210 Results also showed a greater water content for matric potential ranging from  $-10$  hPa ( $\theta_{1.0}$ ) to  
211  $-330$  hPa ( $\theta_{2.5}$ ) for the Syrian dataset. These greater water contents are consistent with the  
212 smaller mean bulk density recorded for the Syrian dataset and a greater proportion of swelling  
213 clays in the Syrian dataset as indicated by the greater mean CEC ( $36.5$  cmol<sub>e</sub>/kg), the OC  
214 content being smaller in Syrian soils and the clay content similar in the two data sets.

### 215 *Evaluation of the continuous- and class-PTFs developed with the French national database*

216 The performance of the continuous- and class-PTFs developed with the French national  
217 database showed that the best prediction was recorded for the French dataset with the class-  
218 PTFs using the water content at field capacity as predictor after stratification by texture (T-  
219 FC-class-PTFs). These class-PTFs are the only ones that perform best for three statistical  
220 criteria (Table 3): the root mean square error (RMSE =  $0.023$  cm<sup>3</sup>/cm<sup>3</sup>) was the smallest and  
221 the precision (SDP =  $0.023$  cm<sup>3</sup>/cm<sup>3</sup>) and coefficient of determination ( $R^2 = 0.81$ ), the greatest  
222 (Table 3) (Fig. 3d). The worst prediction was recorded with the class-PTFs after successive  
223 stratification by texture and bulk density (T-BD-class-PTFs) with the smallest precision (SDP  
224 =  $0.036$  cm<sup>3</sup>/cm<sup>3</sup>) and coefficient of correlation ( $R^2 = 0.52$ ) and the largest root mean square  
225 error (RMSE =  $0.036$  cm<sup>3</sup>/cm<sup>3</sup>) (Table 3) (Fig. 3f). The continuous-PTFs developed for the  
226 parameters of the van Genuchten model (1980) (VG-continuous-PTFs) led to similar results  
227 to those obtained with the T-BD-class-PTFs, with small precision (SDP =  $0.036$  cm<sup>3</sup>/cm<sup>3</sup>) and  
228 high root mean square error (RMSE =  $0.036$  cm<sup>3</sup>/cm<sup>3</sup>) (Table 3) (Fig. 3a).

229 With the Syrian dataset, the best performance was also recorded with the class-PTFs using  
230 water content at field capacity as predictor after stratification by texture (T-FC-class-PTFs)  
231 (Table 3). The estimation bias (MEP =  $-0.001$  cm<sup>3</sup>/cm<sup>3</sup>) and the root mean square error

232 (RMSE = 0.029 cm<sup>3</sup>/cm<sup>3</sup>) were the smallest and the precision (SDP = 0.029 cm<sup>3</sup>/cm<sup>3</sup>) the  
233 greatest, the coefficient of determination ( $R^2 = 0.75$ ) being the second largest with the T-FC-  
234 class-PTFs (Table 3) (Fig. 4d). The worst prediction was recorded with the continuous-PTFs  
235 developed for the parameters of the van Genuchten model (1980) (VG-continuous-PTFs) with  
236 the smallest precision (SDP = 0.046 cm<sup>3</sup>/cm<sup>3</sup>), a high estimation bias (MEP = 0.022 cm<sup>3</sup>/cm<sup>3</sup>)  
237 and the highest root mean square error (RMSE = 0.048 cm<sup>3</sup>/cm<sup>3</sup>) (Table 3) (Fig. 4a). The  
238 class-PTFs after successive stratification by texture and bulk density (T-BD-class-PTFs) gave  
239 results that had rather poor precision and root mean square error, though the estimation bias  
240 was very small (MEP = 0.001 cm<sup>3</sup>/cm<sup>3</sup>) and the coefficient of determination was much  
241 smaller ( $R^2 = 0.51$ ) (Fig. 4f) than with the VG-continuous-PTFs.

242 In accordance with the results published by Cresswell *et al.* (2006), the rather good results  
243 recorded with the class-PTFs that used the water content at field capacity as predictor are  
244 likely related to the fact that the field capacity corresponds to a point on the water retention  
245 curve corresponding to a water potential close to -100 hPa (Al Majou *et al.*, 2008a).  
246 Preliminary stratification by texture increases the prediction quality (Table 3) since the shape  
247 of the WRC and the relative location of the water content corresponding to field capacity on  
248 that curve vary according to texture. Comparison of the performance recorded with the French  
249 and Syrian datasets using the averaged criteria show that the continuous- and class-PTFs  
250 perform better when used for the French dataset (Table 3) which can be considered to be  
251 related to the origin of the soils used to develop the tested PTFs.

252 ***Evaluation of the selected continuous- and class-PTFs from the literature and not using***  
253 ***French soils exclusively***

254 Results recorded with the French dataset show that there was no PTF that performed best for  
255 all four criteria (Table 4). The smallest estimation bias was recorded with the Wösten-

256 continuous-PTFs ( $MEP = -0.002 \text{ cm}^3/\text{cm}^3$ ), the best precision with the Vereecken-  
257 continuous-PTFs ( $SDP = 0.040 \text{ cm}^3/\text{cm}^3$ ), the smallest root mean square error with the  
258 Ghanbarian-continuous-PTFs ( $RMSE = 0.046 \text{ cm}^3/\text{cm}^3$ ) and the greatest correlation  
259 coefficient with the Wösten-class-PTFs ( $R^2 = 0.83 \text{ cm}^3/\text{cm}^3$ ) (Fig. 5a, b, d, g). However, the  
260 performance of the Ghanbarian-continuous-PTFs is among the best except for the correlation  
261 coefficient ( $R^2 = 0.26 \text{ cm}^3/\text{cm}^3$ ) (Table 4) (Fig. 5d).

262 On the other hand, results recorded with the Syrian dataset show that the Wösten-class-PTFs  
263 led to the best results for precision ( $SDP = 0.045 \text{ cm}^3/\text{cm}^3$ ), the smallest root mean squared  
264 error ( $RMSE = 0.047 \text{ cm}^3/\text{cm}^3$ ), the greatest correlation coefficient ( $R^2 = 0.83$ ) but a rather  
265 intermediate prediction bias ( $MEP = 0.019 \text{ cm}^3/\text{cm}^3$ ) (Table 4) (Fig. 6g).

266 Comparison of the results recorded with the French and Syrian datasets using the averaged  
267 criteria show similar performances but much smaller than those recorded with the continuous-  
268 and class-PTFs derived from the French national database (Tables 3 and 4).

### 269 *Evaluation of the performance of the Artificial Neural Networks*

270 The ANN-PTFs developed with the French national database (Fig. 7a) led to a prediction  
271 quality for the French dataset used in this study (Table 5) that was close to the prediction  
272 quality recorded with the best PTFs tested (T-FC-class-PTFs, Table 3) (Fig. 7c). The RMSE  
273 which varies inversely with the overall prediction quality was slightly greater with the ANN  
274 than the one recorded with the T-FC-class-PTFs ( $0.030$  and  $0.023 \text{ cm}^3/\text{cm}^3$ , respectively)  
275 (Tables 3 and 5). The correlation coefficient, which measures the strength of the linear  
276 relation between the predicted and measured water content, was slightly greater with the  
277 ANN-PTFs than with the T-FC-class-PTFs ( $0.85$  and  $0.81$ , respectively). It should also be  
278 mentioned that the prediction quality recorded with the T-FC-class-PTFs was not so far from  
279 the one observed with the ANN-PTFs when applied to the test dataset (20% of the original

280 data, i.e. 91 samples belonging to the French national database) since the RMSE were 0.023  
281 and  $0.029 \text{ cm}^3/\text{cm}^3$ , respectively, and the  $R^2$ , 0.81 and 0.89, respectively (Tables 3 and 5).  
282 On the other hand, the ANN-PTFs developed with the French national database led to a  
283 smaller prediction quality for the Syrian dataset than with the T-FC-class-PTFs developed by  
284 Al Majou *et al.* (2008a). The RMSE recorded with the ANN-PTFs and the T-FC-class-PTFs  
285 was much greater ( $0.049$  and  $0.029 \text{ cm}^3/\text{cm}^3$ , respectively) (Tables 3 and 5) and the  
286 correlation coefficients recorded with the ANN-PTFs slightly greater than with the T-FC-  
287 class-PTFs (0.78 and 0.75, respectively) (Fig. 7b).  
288 The analysis of the results also showed that the PTFs selected in the literature and not using  
289 French soils performed less well than the ANN-PTFs, as already reported in the literature  
290 (Nguyen *et al.*, 2017) (Tables 4 and 5). The RMSE and  $R^2$  were respectively greater and  
291 smaller than with the ANN-PTFs, using the PTFs selected in the literature and not using  
292 French soils. The Wösten-class-PTFs had however a much higher correlation coefficient ( $R^2$   
293 = 0.83 for the French and Syrian datasets) than that recorded for the other PTFs selected in the  
294 literature and fairly similar to the correlation coefficient recorded with the ANN (Tables 4 and  
295 5).

296

## 297 **Conclusion**

298 Our results show that PTFs developed for French soils are transferable to the Syrian soils  
299 selected for this study of semiarid Mediterranean soils. With the class-PTFs which use the soil  
300 water content at field capacity as predictor after stratification by texture, the quality of  
301 prediction is similar to that recorded with ANNs which are nowadays recognized as leading to  
302 a quality of prediction better or similar to those recorded with the PTFs published in the  
303 literature. The performance of these PTFs can be explained by the fact that a point on the  
304 water retention curve is actually used as a predictor even if the attribution of an accurate water

305 potential value to the field capacity state is not possible. Stratification by texture prior to the  
306 development of these PTFs then increases their ability to predict the water retention properties  
307 properly, as the shape of the water retention curve is closely related to the soil texture. In  
308 other words, the performance of the class-PTFs which use the field water content as predictor  
309 after stratification by texture is likely related to using information about both the elementary  
310 particle size distribution (texture) and their assemblage (structure and related porosity) which  
311 are known to be major basic soil properties responsible for variability in water retention  
312 properties. When the soil water content at field capacity is not available, the best performance  
313 recorded remains less clear. If the coefficient of determination recorded with continuous-PTFs  
314 is large when using texture information as predictor, the bias is large when applied to Syrian  
315 soils. With a lower coefficient of determination but the other statistical criteria close to those  
316 recorded when using water content at field capacity as predictor, our results show that worthy  
317 results in terms of transferability potential were recorded with class-PTFs using bulk density  
318 as predictor after stratification by texture.

319 Analysis of the performance recorded with the continuous- and class-PTFs selected in the  
320 literature shows a poorer quality of prediction than PTFs developed with French soils. This  
321 probably has nothing to do with the origin of the soils but with a more appropriate  
322 consideration of soil characteristics related to soil composition and structure. The high  
323 correlation coefficients recorded with the class-PTFs developed by Wösten *et al.* (1999) and  
324 Shaap *et al.* (2001) are therefore likely related to their use of stratification by texture, thus  
325 leading to a high consistency of the water content variation according to water potential even  
326 if the prediction bias and prediction accuracy are high and low, as shown by the MEP and  
327 SDP, respectively.

328 Finally, our results show that continuous- or class-PTFs could be considered as transferable  
329 with satisfactory performance to other countries where database of hydraulic soil properties

330 are not available to establish their own PTFs. The expected prediction quality of the PTFs  
331 transferred appeared to be mainly related to their ability to take into account predictors related  
332 to the characteristics of the elementary particles and their assemblage, since the best results  
333 were recorded with PTFs which combine predictors related to both soil composition and  
334 structure. Our results also showed that taking into account several predictors related to soil  
335 composition together (particle size distribution, texture, organic carbon content) and soil  
336 structure together (bulk density, porosity, field capacity) does not lead to a better performance  
337 and subsequently to the best transferability potential. It is noteworthy that the best  
338 performance were recorded by the class-PTFs that use texture as stratification criteria and  
339 then the water content at field capacity as structure information.

#### 340 **Acknowledgement**

341 The authors would like to thank the Embassy of France in Damascus, and the Francophone  
342 University Agency (AUF) for supporting scientific collaboration between France and Syria.  
343 The first author also received funding support from the Labex Voltaire (ANR-10-LABEX-  
344 100-01) and the French program PAUSE.

345

#### 346 **References**

347 Adhikary, P.P., Chakraborty, D., Kalra, N., Sachdev, C.B., Patra, A.K., Kumar, S., Tomar,  
348 R.K., Chandna, P., Raghav, D., Agrawal, K. & Sehgal, M. 2008. Pedotransfer functions for  
349 predicting the hydraulic properties of Indian soils. *Australian Journal of Soil Research*. **46**,  
350 476–484.

351 Al Majou, H., Bruand, A., Duval, O. & Cousin, I. 2007. Variation of the water retention  
352 properties of soils: validity of class-pedotransfer functions. *Comptes Rendus Geoscience*,  
353 **339**, 632–639.



354 Al Majou, H., Bruand, A. & Duval, O. 2008a. Use of in situ volumetric water content at field  
355 capacity to improve prediction of soil water retention properties. *Canadian Journal of Soil*  
356 *Science*, **88**, 533–541.

357 Al Majou, H., Bruand, A., Duval, O., Le Bas, C. & Vautier, A. 2008b. Prediction of soil water  
358 retention properties after stratification by combining texture, bulk density and the type of  
359 horizon. *Soil Use and Management*, **24**, 383–391.

360 Baker, L. 2008. Development of class pedotransfer functions of soil water retention - A  
361 refinement. *Geoderma*, **144**, 225–230.

362 Baize, D. 2000. Guide des analyses en pédologie. INRA Paris.

363 Bouma, J., 1989. Using soil survey data for quantitative land evaluation. *Advances in Soil*  
364 *Science*, **9**, 177–213.

365 Børgesen, C.D. & Schaap, M.G. 2005. Point and parameter pedotransfer functions for water  
366 retention predictions for Danish soils. *Geoderma*, **127**, 154–167,

367 Bruand, A. & Tessier, D. 2000. Water retention properties of the clay in soils developed on  
368 clayey sediments: Significance of parent material and soil history. *European Journal of*  
369 *Soil Science*, **51**, 679–688.

370 Bruand, A., Pérez Fernandez, P. & Duval, O. 2003. Use of class pedotransfer functions based  
371 on texture and bulk density of clods to generate water retention curves. *Soil Use and*  
372 *Management*, **19**, 232–242.

373 Ciesielski, H. & Sterckeman, T. 1997. Determination of cation exchange capacity and  
374 exchangeable cations in soils by means of cobalt hexamine trichloride. Effects of  
375 experimental conditions. *Agronomie*, **17**, 1-7.

376 Commission of the European Communities (CEC). 1985. Soil map of the European  
377 Communities. Scale 1:1000000. CEC-DGVI, Luxembourg.

378 Cornelis, W.M., Ronsyn, J., Van Meirvenne, M. & Hartmann, R. 2001. Evaluation of  
379 pedotransfer functions for predicting the soil moisture retention curve. *Soil Science Society*  
380 *of America Journal*, **65**, 638–648.

381 Cresswell, H.P., Coquet, Y., Bruand, A. & Mckenzie, N.J. 2006. The transferability of  
382 Australian pedotransfer functions for predicting water retention characteristics of French  
383 soils. *Soil Use and Management*, **22**, 62–70.

384 Demuth, H. & Beale, M. 2000. Neural Network Toolbox for Use with MATLAB, User  
385 Guide. The MathWorks, Inc. Natick, MA.

386 Dridi, B. & Dilmi, A. 2011. Poids des différentes caractéristiques des sols dans l'estimation  
387 de leur rétention en eau. *Etude et Gestion des Sols*, **18**, 247–258.

388 Dupuis, M. 1969. Dosage des carbonates dans les fractions granulométriques de quelques sols  
389 calcaires et dolomitiques. *Annales Agronomiques*, **20**, 1, 61-88.

390 Fashi, F.H. 2014. Evaluation of artificial neural network and regression PTFs in estimating  
391 some soil hydraulic parameters. *ProEnvironment*, **7**, 10-20.

392 Food and Agriculture Organization (FAO), 1990. Guidelines for soil description (3<sup>rd</sup> ED.).  
393 FAO/ISRIC. Rome.

394 van Genuchten, M.Th. 1980. A closed-form equation for predicting the hydraulic conductivity  
395 of unsaturated soil. *Soil Science Society of America Journal*, **44**, 892–898.

396 Ghorbani, D.G.S., Homae, M. & Khodaverdilo, H. 2010. Derivation and validation of  
397 pedotransfer functions for estimating soil water retention curve using a variety of soil data.  
398 *Soil Use and Management*. **26**, 68–74.

399 Ghanbarian-Alavijeh, B. & Millán, H. 2010. Point pedotransfer functions for estimating soil  
400 water retention curve. *International Agrophysics*, **24**, 243–251.

401 Haghverdi, A., Cornelis, W.M. & Ghahraman, B. 2012. A pseudo-continuous neural network  
402 approach for developing water retention pedotransfer functions with limited data. *Journal*  
403 *of Hydrology*, **442-443**, 46–54.

404 Haghverdi, A., Leib, B.G. & Cornelis W.M. 2015. A simple nearest-neighbor technique to  
405 predict the soil water retention curve. *American Society of Agricultural and Biological*  
406 *Engineers*, **58**, 3, 697–705.

407 Haykin, S. 1994. Neural networks, a comprehensive foundation, 1st ed. *Macmillan College*  
408 *Publishing*, New York, NY.

409 Hodnett, M.G. & Tomasella, J. 2002. Marked differences between van Genuchten soil water-  
410 retention parameters for temperate and tropical soils: A new water-retention pedotransfer  
411 function developed for tropical soils. *Geoderma*, **108**, 155–180.

412 ISSS Working Group RB, 1998. World Reference Base for Soil Resources: Introduction. J.A.  
413 Deckers, F.O. Nachtergaele & O.C. Spaargaren Eds. First edition. ISSS, ISRIC & FAO.  
414 Acco, Leuven.

415 Khlosi, M., Cornelis, W.M., Douaik, A., Hazzouri, A., Habib, H. & Gabriels, D. 2013.  
416 Exploration of the Interaction between Hydraulic and Physicochemical Properties of  
417 Syrian Soils. *Vadose Zone Journal*, **12**, 4, 1–11.

418 Khlosi, M., Alhamdoosh, M., Douaik, A., Gabriels, D. & Cornelis, W.M. 2016. Enhanced  
419 pedotransfer functions with support vector machines to predict water retention of  
420 calcareous soil. *European Journal of Soil Science*, **67**, 276–284.

421 Ilaiwi, M. 1980. ACSAD report on soil of Syria and Lebanon scale 1:1000000.

422 Lamorski, K., Pachepsky, Y.A., Slawinski, C. & Walczak, R. 2008. Using support vector  
423 machines to develop pedotransfer functions for water retention of soils in Poland. *Soil*  
424 *Science Society of America Journal*, **72**, 1243–1247.

425 Land Classification and Soil Survey of the Syrian Arab Republic, 1982. (Reconnaissance Soil  
426 Survey of Syria, 1: 500,000). Louis Berger International Inc., Remote Sensing Institute  
427 South Dakota University, United States Agency for International Development,  
428 *Washington DC, 2.*

429 van Liere, W.J. 1995. Classification and rational utilization of soils. Report to the  
430 Government of Syria. FAO, Rome, 151p.

431 Lilly, A., Wosten, J.H.M., Nemes, A. & Le Bas, C. 1999. The development and use of the  
432 HYPRES database in Europe. In: MTh van Genuchten & FJ Leij, Eds, Characterization  
433 and measurement of the hydraulic properties of unsaturated porous media. *Proceedings of*  
434 *the International Workshop, Riverside, California, October 22–24, 1283–1294.*

435 Medeiros, J.C., Cooper, M., Dalla, R.J., Grimaldi, M. & Coquet, Y. 2014. Assessment of  
436 pedotransfer functions for estimating soil water retention curves for the amazon region.  
437 *Revista Brasileira de Ciência do Solo, 38, 3, 730-743.*

438 Medrado, E. & Lima, J.E.F.W. 2014. Development of pedotransfer functions for estimating  
439 water retention curve for tropical soils of the Brazilian savanna. *Geoderma Regional, 1,*  
440 *55–66.*

441 Minasny B., Hopmans, J.W. Harter, T. Eching, S.O. Tuli, A. & Denton, M.A. 2004. Neural  
442 networks prediction of soil hydraulic functions for alluvial soils using multistep outflow  
443 data. *Soil Science Society of America Journal, 68, 417–429.*

444 Minasny, B., & Hartemink, A.E. 2011. Predicting soil properties in the tropics. *Earth Science*  
445 *Reviews, 106, 52–62.*

446 Mohawesh, O. 2013. Assessment of pedotransfer functions (PTFs) in predicting soil hydraulic  
447 properties under arid and semi-arid environments. *Journal of Agriculture Sciences, 9, 475–*  
448 *492.*

449 Mrabet, R. 2011. Climate change and carbon sequestration in the Mediterranean basin:  
450 Contributions of no-tillage systems. 4<sup>ème</sup> Rencontres Méditerranéennes du Semis Direct,  
451 *Options Méditerranéennes*, 165-184.

452 Nasta, P., Kamai, T., Chirico, G.B., Hopmans, J. & Romano. R. 2009. Scaling soil water  
453 retention functions using particle-size distribution. *Journal of Hydrology*, **374**, 223–234.

454 Nemes, A. 2002. Unsaturated soil hydraulic database of Hungary: HUNSODA, *Agrokémia és*  
455 *Talajtan*, **51**, 17–26.

456 Nemes A., Schaap, M.G. & Wösten, J.H.M. 2002. Validation of international scale soil  
457 hydraulic pedotransfer functions for national scale applications. International Symposium  
458 n° 04 on 17th WCSS, poster presentation, 14–21 August, Thailand.

459 Nemes, A., Schaap, M.G. & Wösten, J.H.M. 2003. Functional evaluation of pedotransfer  
460 functions derived from different scales of data collection. *Soil Science Society of America*  
461 *Journal*, **67**, 1093–1102.

462 Nemes, A., Rawls, W. J. & Pachepsky, Y.A. 2006a. Use of the nonparametric nearest  
463 neighbor approach to estimate soil hydraulic properties. *Soil Science Society of America*  
464 *Journal*, **70**, 327–336.

465 Nemes, A. 2015. Why do they keep rejecting my manuscript-do's and don'ts and new  
466 horizons in pedotransfer studies? *Agrokémia És Talajtan*, **64**, 361–371.

467 Nguyen, P.M., J. De Pue., K.V. Le. & Cornelis, W.M. 2015. Impact of regression methods on  
468 improved effects of soil structure on soil water retention estimates. *Journal of Hydrology*,  
469 **525**, 598–606.

470 Nguyen, P.M., Haghverdi, A., Pue, J. De., Botula, Y. D., Khoa V. Le, Waegeman, W. &  
471 Cornelis W.M. 2017. Comparison of statistical regression and data-mining techniques in  
472 estimating soil water retention of tropical delta soils. *Biosystems Engineering*, **153**, 12–27.

473 Pachepsky, Y.A., Timlin, D. & Varallyay, G. 1996. Artificial neural networks to estimate soil  
474 water retention from easily measurable data. *Soil Science Society of America Journal*, **60**,  
475 727–733.

476 Pachepsky, Y.A. & Rawls, W.J. 1999. Accuracy and reliability of pedotranfer functions as  
477 affected by grouping soils. *Soil Science Society of America Journal*, **63**, 1748-1757.

478 Pachepsky, Y.A., Rawls, W.J. & Lin, H.S. 2006. Hydropedology and pedotransfer functions.  
479 *Geoderma*, **131**, 308–316.

480 Patil, N.G., Pal, D.K., Mandal, C. & Mandal, D.K. 2012. Soil water retention characteristics  
481 of vertisols and pedotransfer functions based on nearest neighbor and neural networks  
482 approaches to estimate AWC. *Journal of Irrigation and Drainage Engineering*, **138**, 2,  
483 177–184.

484 Ramos, T.B., Goncalves, M.C., Brito, D., Martins, J.C. & Pereira, L.S., 2013. Development of  
485 class pedotransfer functions for integrating water retention properties into Portuguese soil  
486 maps. *Soil Research*, 51, 4, 262–277.

487 Reichert, J. M., Albuquerque, J. A., Kaiser, A. R., Reinert, D. J., Urach, F. L. & Carlesso, R.  
488 2009. Estimation of water retention and availability in soils of Rio Rrande Do Sul. *Revista*  
489 *Brasileira de Ciência do Solo*, **33**, 1547–1560.

490 Rigot, J-B., 2006. L'évolution ralentie du milieu naturel dans la steppe aride du nord de la  
491 Syrie à l'Holocène. *Géomorphologie: Relief, Processus, Environnement*, **4**, 259–274.

492 Robert, M. & Tessier D. 1974. Méthode de préparation des argiles des sols pour les études  
493 minéralogiques. *Annales Agronomiques*, **25**, 859–882.

494 Santra, P., Das, B.S. 2008. Pedotransfer functions for soil hydraulic properties developed  
495 from a hilly watershed of Eastern India. *Geoderma*, **146**, 439–448.

496 Schaap, M.G., Leij, F.J. & van Genuchten, Th.M. 2001. ROSETTA: A computer program for  
497 estimating soil hydraulic parameters with hierarchical pedotransfer functions. *Journal of*  
498 *Hydrology*, **251**, 163–176.

499 Schaap, M.G. & Bouten, W., 1996. Modelling water retention curves of sandy soils using  
500 neural networks. *Water Resources Research*, **32**, 3033–3040.

501 Schaap, M.G., 2004. Accuracy and uncertainty in PTF predictions. In: Y. Pachepsky, W.J.  
502 Rawls (eds) Development of Pedotransfer Functions in Soil Hydrology. *Development in*  
503 *Soil Science*, **30**, 33–43.

504 Schaap, M.G., Leij, F. J. & van Genuchten, M. Th. 2001. Rosetta: A computer program for  
505 estimating soil hydraulic parameters with hierarchical pedotransfer functions. *Journal of*  
506 *Hydrology*, **251**, 163–176.

507 Sommer, R., Piggini, C., Haddad, A., Hajdibo, A., Hayek, P. & Khalil, Y. 2012. Simulating  
508 the effects of zero tillage and crop residue retention on water relations and yield of wheat  
509 under rainfed semiarid Mediterranean conditions. *Field Crops Research*, **132**, 40–52.

510 Touil, S., Degré, A. & Chabaka M.N. 2016. Transposability of pedotransfer functions for  
511 estimating water retention of Algerian soils. *Desalination and Water Treatment*, **57**, 12,  
512 5232–5240.

513 Tomasella, J., Pachepsky, Y.A., Crestana S. & Rawls J. 2003. Comparison of Two  
514 Techniques to Develop Pedotransfer Functions for Water Retention. *Soil Science Society of*  
515 *America Journal*, **67**, 1085–1092.

516 Twarakavi, N. K. C., Simonek, J., & Schaap, M. 2009. Development of pedotransfer  
517 functions for estimation of soil hydraulic parameters using support vector machines. *Soil*  
518 *Science Society of America Journal*, **73**, 1443–1452.

519 Vereecken, H., Maes, J., Feyen, J. & Darius, P. 1989. Estimating the soil moisture retention  
520 characteristics from texture, bulk density and carbon content. *Soil Science*, **148**, 389–403.

- 521 Wösten J.H.M., Schuren, C.H.J.E., Bouma, J. & Stein, A. 1990. Functional sensitivity  
522 analysis of four methods to generate soil hydraulic functions. *Soil Science Society of*  
523 *America Journal*, **54**, 832-836.
- 524 Wösten J.H.M., Finke P.A. & Jansen M.J.W. 1995. Comparison of class and continuous  
525 pedotransfer functions to generate soil hydraulic characteristics. *Geoderma*, **66 (3-4)**, 227–  
526 237.
- 527 Wösten, J.H.M., Lilly, A., Nemes, A. & Le Bas, C. 1999. Development and use of a database  
528 of hydraulic properties of European soils. *Geoderma*, **90**, 169–185.
- 529 Wösten, J.H.M., Pachepsky, Y.A. & Rawls, W.J. 2001. Pedotransfer functions: bridging the  
530 gap between available basic soil data missing soil hydraulic characteristics. *Journal of*  
531 *Hydrology*, **251**, 123–150.
- 532 Wösten, J.H.M., Verzandvoort, S.J.E., Leennaars, J.G.B., Hoogland, T. & Wesseling, J.G.  
533 2013. Soil hydraulic information for river basin studies in semi-arid regions. *Geoderma*,  
534 **195-196**, 79–86.
- 535 Yuksel, H. 1982. Land classification/soil survey project of the Syrian Arab Republic. Contract  
536 USAID-C-1644.



537 Table 1  
 538 List of continuous- and class-PTFs according to the output variables and relationship between input and output variables.

Output variables	Relationship between input and output variables (continuous-PTFs) and stratification type (class-PTFs)	Input variables	Geographical domain or country	Reference	
<b>Continuous-PTF</b>					
Parameters of a water retention curve model	MLR	PSD, BD, OC	Belgium	Vereecken <i>et al.</i> (1989)	
		PSD, BD, OM	Europe	Wösten <i>et al.</i> (1999)	
		PSD, BD, OC, pH, CEC	Tropics	Hodnett & Tomasella (2002)	
		PSD, BD, Me	Brazil	Tomasella <i>et al.</i> (2003)	
		PSD	India	Adhikary <i>et al.</i> (2008)	
		PSD, BD, OC	France	Al Majou <i>et al.</i> (2008a)	
		PSD, OC, pH	India	Santra & Das (2008)	
		PSD, BD, $d_g$ , $\sigma_g$	Iran	Ghorbani <i>et al.</i> (2010)	
		PSD, BD, OC	India	Patil <i>et al.</i> (2012)	
		PSD, BD, OM	Brazil	Medrado & Lima, (2014)	
		ANN	PSD, BD, $\theta_{33}$ , $\theta_{1500}$	North America, Europe	Schaap <i>et al.</i> (2001)
			PSD, BD, OM, $\theta_1$ , $\theta_{10}$ , $\theta_{100}$ , $\theta_{1500}$	Denmark	Børgesen & Schaap (2005)
			PSD, BD, OC, $\log(h)$	Iran, Australia	Haghverdi <i>et al.</i> (2012)
	SVM	PSD, BD, $\log(h)$	USA	Twarakavi <i>et al.</i> (2009)	
Set of $\theta$ at different water potentials	MLR and LR	PSD, BD, Me	Brazil	Tomasella <i>et al.</i> (2003)	
		$\theta_{FC}$	France	Al Majou <i>et al.</i> (2008a)	
		PSD, BD, OM	Brazil	Reichert <i>et al.</i> (2009)	
		PSD, BD, $d_g$ , $\sigma_g$ , $\theta(h)$	USA, France	Ghanbarian & Millán (2010)	
		PSD, BD, $d_g$ , $\sigma_g$	Iran	Ghorbani <i>et al.</i> (2010)	
		PSD, BD, OC	Tropics, USA	Minasny & Hartemink (2011)	
		PSD, BD, OM, PL	Syria	Khlosi <i>et al.</i> (2016)	
		PSD, BD, OC, $\log(h)$	Vietnam	Nguyen <i>et al.</i> (2017)	
		ANN	PSD, BD, OM, $\theta_1$ , $\theta_{10}$ , $\theta_{100}$ , $\theta_{1500}$	Denmark	Børgesen & Schaap (2005)
			PSD, BD	Poland	Lamorski <i>et al.</i> (2008)
			PSD, BD, OC, $\log(h)$	Iran, Australia	Haghverdi <i>et al.</i> (2012)
			PSD, BD, OC	India	Patil <i>et al.</i> (2012)
			PSD, BD, OM, PL	Syria	Khlosi <i>et al.</i> (2016)
	PSD, BD, OC, $\log(h)$	Vietnamese	Nguyen <i>et al.</i> (2017)		
	SVM	PSD, BD	Poland	Lamorski <i>et al.</i> (2008)	

k-NN	PSD, BD, OC	Vietnam	Nguyen <i>et al.</i> (2015)
	PSD, BD, OM, PL	Syria	Khlosi <i>et al.</i> (2016)
	PSD, BD, OC, $\log(h)$	Vietnam	Nguyen <i>et al.</i> (2017)
	PSD, BD, OM	USA	Nemes <i>et al.</i> (2006a)
	PSD, BD, OC	India	Patil <i>et al.</i> (2012)
	PSD, BD	USA, Belgium	Haghverdi <i>et al.</i> (2015)
	PSD, BD, OC	Vietnam	Nguyen <i>et al.</i> (2015)
PSD, BD, OC, $\log(h)$	Vietnam	Nguyen <i>et al.</i> (2017)	

### Class-PTF

Parameters of a water retention curve model	Multiple parameters class distribution	T, Hor.	Europe	Wösten <i>et al.</i> (1999)
		T, Hor.	Tropics	Hodnett & Tomasella (2002)
		T, Hor.	France	Al Majou <i>et al.</i> (2007)
		T, Hor.	France	Al Majou <i>et al.</i> (2008a)
	Mono parameter class distribution	T	North America, Europe	Schaap <i>et al.</i> (2001)
Set of $\theta$ at different water potentials	Multiple parameter class distribution	T, BD	France	Bruand <i>et al.</i> (2003)
		T, BD, Hor.	France	Al Majou <i>et al.</i> (2008b)
		Statistical distribution of dataset (texture, horizon)	Europe	Baker (2008)
	Mono parameter class distribution	T, BD, Hor.	Portugal	Ramos <i>et al.</i> (2013)
		T, FC	France	Al Majou <i>et al.</i> (2008a)
		T	France	Al Majou <i>et al.</i> (2008b)

539 MLR : multiple linear regression, LR: linear regression, ANN: artificial neural networks, SVM: support vector machine, k-NN: k nearest neighbor technique, PSD: particle size distribution, BD:  
540 bulk density, OC: organic carbon, OM: organic matter, CEC: cation exchange capacity, Me: moisture equivalent,  $d_g$ : geometric mean particle size diameter,  $\sigma_g$ : geometric standard deviation, PL:  
541 plastic limit,  $\theta_{FC}$ : volumetric water content at field capacity,  $\theta_{(1, 10, 33, 100, 1500)}$  volumetric water content at matric potential (kPa),  $\log(h)$ : logarithm of the absolute value of matric head in cm water, T:  
542 texture class, Hor: type of horizon (topsoil or subsoil).  
543

544 Table 2

545 Descriptive statistics of main characteristics of the soil dataset used in this study.

	Coarse elements	Particle size distribution			OC	CaCO <sub>3</sub>	CEC	D <sub>b</sub>	Volumetric water content (cm <sup>3</sup> /cm <sup>3</sup> ) at matric potential h ( $\theta_h$ ) in						
	(%)	(%)							g/kg	g/kg	Cmol <sub>c</sub> /kg	g/cm <sup>3</sup>	hPa		
	>2000	<2	2-50	50-2000					$\theta_{10}$	$\theta_{33}$	$\theta_{100}$	$\theta_{330}$	$\theta_{1000}$	$\theta_{3300}$	$\theta_{15000}$
	$\mu\text{m}$	$\mu\text{m}$	$\mu\text{m}$	$\mu\text{m}$											
French National database used to train and test the PTFs (n = 456)															
mean	<1	29.3	43.8	26.9	6.0	54.2	14.8	1.52	0.354	0.335	0.315	0.289	0.259	0.221	0.187
s.d.	–	15.4	21.8	25.6	5.1	171.3	9.0	0.15	0.068	0.070	0.075	0.076	0.079	0.076	0.073
min.	–	1.9	1.6	0.1	0.0	0.0	0.6	0.95	0.134	0.100	0.080	0.056	0.045	0.033	0.013
max.	–	92.9	82.1	95.4	28.8	982	52.8	1.98	0.605	0.596	0.586	0.557	0.510	0.462	0.370
French soil samples used to test the PTFs (n = 30)															
mean	<1	42.1	32.0	25.9	8.58	34.30	22.03	1.45	0.387	0.365	0.347	0.326	0.307	0.274	0.244
s.d.	–	14.4	13.7	15.1	6.8	98.5	10.1	0.16	0.049	0.050	0.051	0.054	0.055	0.050	0.058
min.	–	20.1	10.5	3.1	0.0	0.0	5.30	1.10	0.310	0.295	0.275	0.242	0.203	0.167	0.142
max.	–	68.9	53.5	59.8	28.8	424	45.90	1.77	0.496	0.489	0.469	0.446	0.415	0.366	0.363
Syrian soil samples used to test the PTFs (n = 30)															
mean	<1	41.4	32.8	27.8	1.18	63.7	36.5	1.22	0.436	0.417	0.388	0.344	0.307	0.277	0.239
s.d.	–	16.0	9.8	11.7	0.96	77.9	7.3	0.10	0.061	0.058	0.055	0.050	0.051	0.062	0.067
min.	–	12.2	11.6	8.0	0.36	7.2	23.7	1.04	0.352	0.341	0.324	0.285	0.242	0.198	0.149
max.	–	69.1	53.3	53.0	3.9	310	49.2	1.41	0.577	0.559	0.507	0.474	0.444	0.435	0.404

546 s.d., min, max are the standard deviation, minimum and maximum of soil variables.

547

548

549

550

551

552

553 Table 3  
 554 Validation criteria of the continuous-PTFs and class-PTFs developed with the French national  
 555 database when applied to the French and Syrian datasets.

PTFs type	Descriptive statistics of the relationship between measured and predicted water content			
	MEP (cm <sup>3</sup> /cm <sup>3</sup> )	SDP (cm <sup>3</sup> /cm <sup>3</sup> )	RMSE (cm <sup>3</sup> /cm <sup>3</sup> )	R <sup>2</sup>
French dataset (n=30)				
VG-continuous-PTFs	-3*10 <sup>-4</sup>	0.036	0.036	0.77
PSD-continuous-PTFs	-0.003	0.033	0.033	0.81
FC-continuous-PTFs	-0.012	0.028	0.031	0.66
T-FC-class-PTFs	-0.001	0.023	0.023	0.81
T-class-PTFs	-0.002	0.028	0.028	0.71
T-BD-class-PTFs	0.003	0.036	0.036	0.52
T-BD-H-class-PTFs	-0.002	0.029	0.029	0.69
T-H-VG-class-PTFs	-0.003	0.030	0.030	0.68
Average	0.003*	0.030	0.031	0.71
Syrian dataset (n=30)				
VG-continuous-PTFs	0.022	0.046	0.048	0.74
PSD-continuous-PTFs	-0.021	0.033	0.035	0.85
FC-continuous-PTFs	-0.005	0.033	0.034	0.66
T-FC-class-PTFs	-0.001	0.029	0.029	0.75
T-class-PTFs	-0.025	0.039	0.047	0.36
T-BD-class-PTFs	0.001	0.041	0.041	0.51
T-BD-H-class-PTFs	0.002	0.039	0.039	0.56
T-H-VG-class-PTFs	-0.024	0.037	0.044	0.43
Average	0.013*	0.037	0.040	0.61

556 \*: Computed using the absolute value of every MEP. VG-continuous-PTFs are the continuous pedotransfer functions developed for the  
 557 parameters of the van Genuchten model using multiple regression equations, PSD-continuous-PTFs are the continuous pedotransfer  
 558 functions developed by multiple regression equations using particle-size distribution (PSD), organic carbon and bulk density, FC-continuous-  
 559 PTFs are the continuous pedotransfer functions developed by using the water content at field capacity, T-FC-class-PTFs are the class  
 560 pedotransfer functions developed by using the water content at field capacity as predictor after stratification by texture., T-class-PTFs are the  
 561 pedotransfer functions developed after stratification by texture, T-BD-class-PTFs are the pedotransfer functions developed after stratification  
 562 by texture and bulk density, T-BD-H-class-PTFs are the pedotransfer functions developed for texture and bulk density classes according to  
 563 the type of horizon, T-H-VG-class-PTFs are the pedotransfer functions developed after stratification by texture and type of horizon (topsoil  
 564 and subsoil) for the parameters of the van Genuchten model (1980).

565  
 566  
 567  
 568  
 569  
 570  
 571  
 572  
 573  
 574

575 Table 4  
 576 Criteria enabling assessment of the prediction quality for the continuous- and class-PTFs  
 577 selected in the literature and not using the French national database.

PTFs type	Descriptive statistics of the relationship between measured and predicted water content			
	MEP (cm <sup>3</sup> /cm <sup>3</sup> )	SDP (cm <sup>3</sup> /cm <sup>3</sup> )	RMSE (cm <sup>3</sup> /cm <sup>3</sup> )	R <sup>2</sup>
	French dataset (n=30)			
Wösten-continuous-PTFs	-0.002	0.051	0.051	0.30
Vereecken-continuous-PTFs	0.038	0.040	0.055	0.21
Reichert-continuous-PTFs	0.031	0.042	0.052	0.12
Ghanbarian-continuous-PTFs	0.005	0.045	0.046	0.26
Minasny-continuous-PTFs	0.016	0.051	0.054	0.20
Schaap-class-PTFs	-0.019	0.072	0.075	0.60
Wösten-class-PTFs	0.040	0.050	0.064	0.83
Average	0.022*	0.050	0.057	0.36
	Syrian dataset (n=30)			
Wösten-continuous-PTFs	0.005	0.059	0.059	0.43
Vereecken-continuous-PTFs	0.022	0.052	0.052	0.20
Reichert-continuous-PTFs	-0.020	0.044	0.048	0.42
Ghanbarian-continuous-PTFs	-0.006	0.051	0.051	0.21
Minasny-continuous-PTFs	0.003	0.050	0.050	0.30
Schaap-class-PTFs	-0.048	0.056	0.074	0.76
Wösten-class-PTFs	0.019	0.043	0.047	0.83
Average	0.018*	0.051	0.054	0.45

578 \*: Computed using the absolute value of every MEP

579

580

581

582

583

584

585

586

587

588

589

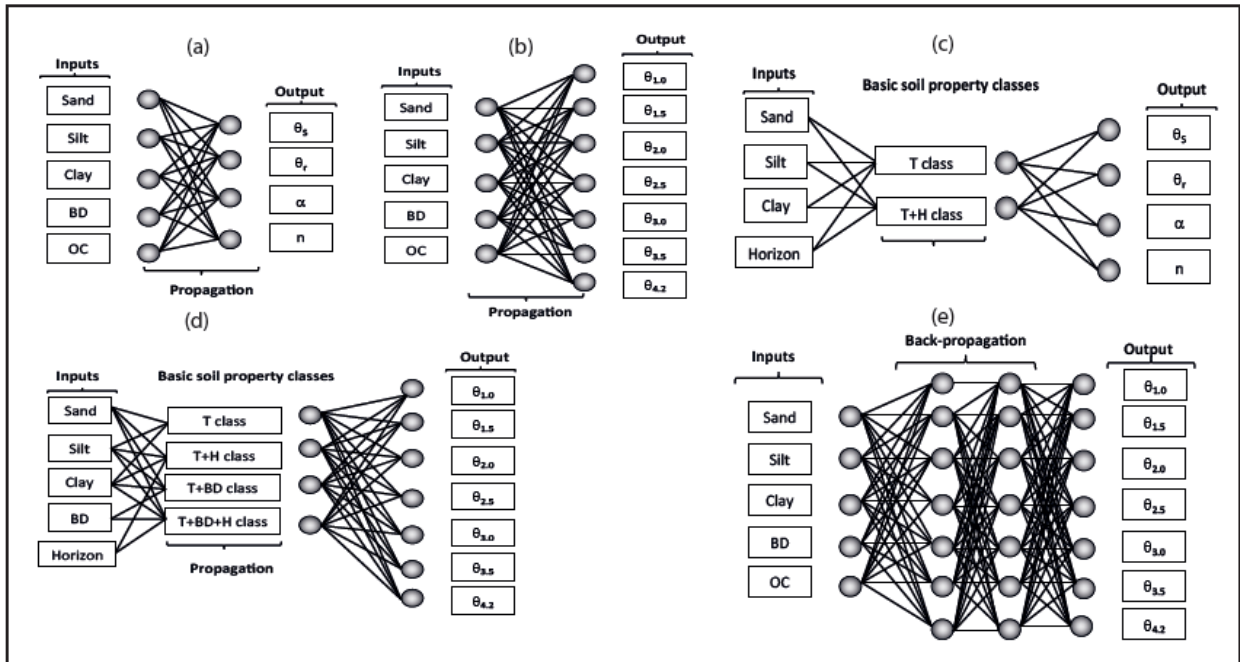
590

591 Table 5  
 592 Descriptive statistics of the relationship between measured and predicted water content  
 593 developed by artificial neural networks (ANN).

	Training data		Test data	
	RMSE (cm <sup>3</sup> /cm <sup>3</sup> )	<i>R</i> <sup>2</sup>	RMSE (cm <sup>3</sup> /cm <sup>3</sup> )	<i>R</i> <sup>2</sup>
French National database	0.030	0.90	0.029	0.89
Syrian dataset	-	-	0.049	0.78
French dataset	-	-	0.030	0.85

594 Soil properties used in predictive procedures are the sand, silt, clay and organic carbon contents, and the bulk density.  
 595  
 596

597

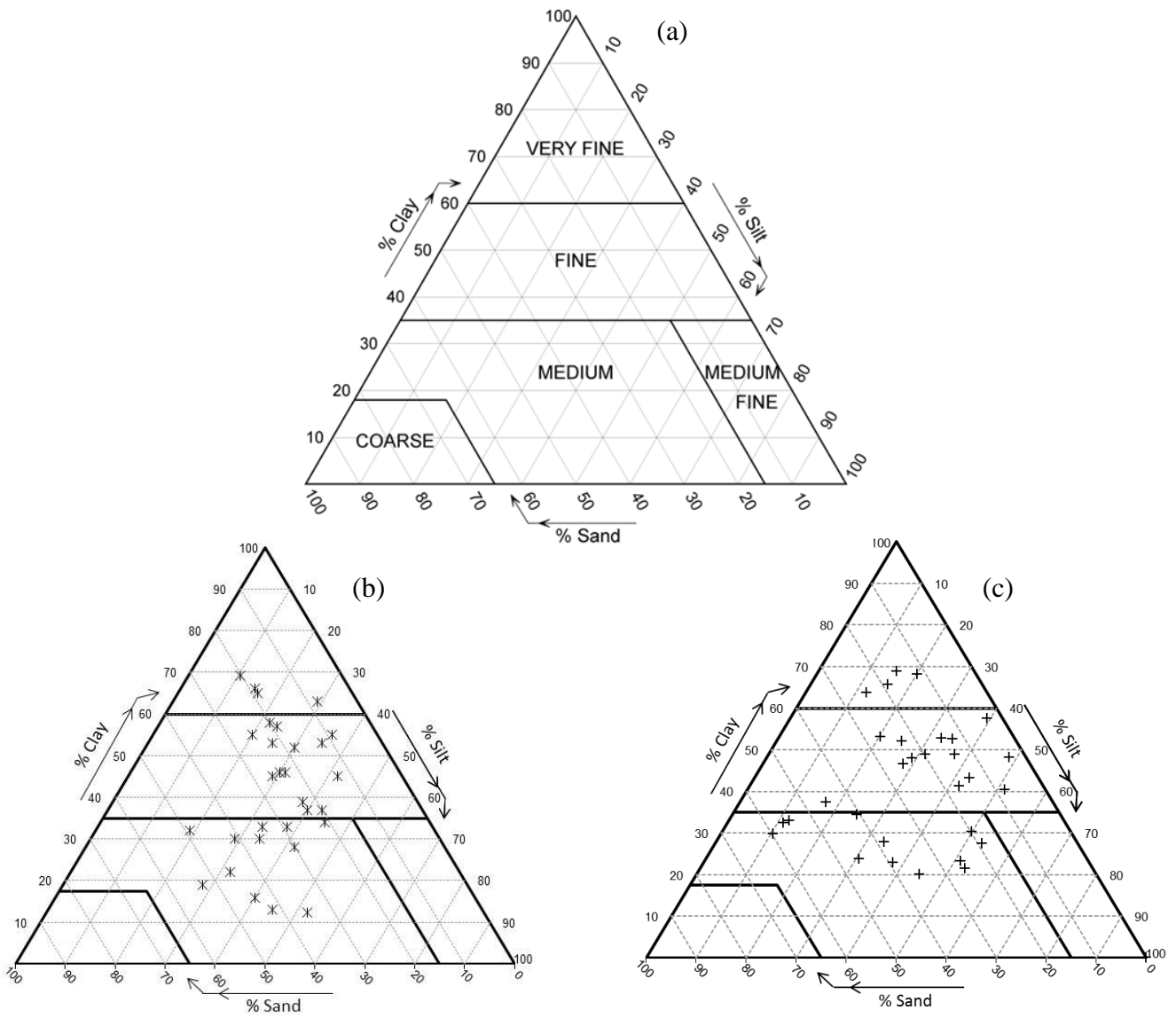


599  
 600  
 601  
 602  
 603  
 604  
 605  
 606  
 607  
 608  
 609

**Figure 1:** The typical topologies of the continuous and class-PTFs used in this study. (a): continuous-PTFs providing the parameters of the van Genuchten model (1980), (b): continuous-PTFs providing the water content at several matric potentials, (c): class-PTFs providing the parameters of the van Genuchten model (1980), (d): class-PTFs providing the water content at several matric potentials, and (e): artificial neural networks (ANN)-PTFs.  $\theta_1, \theta_{1.5}, \dots, \theta_{4.2}$ : volumetric water content in  $\text{cm}^3 \text{cm}^{-3}$  at seven different matric potentials,  $\theta_r, \theta_s, \alpha$  and  $n$  are the parameters of the van Genuchten equation, T: texture, BD: bulk density, OC: organic carbon, H: type of horizon (topsoil or subsoil).

610

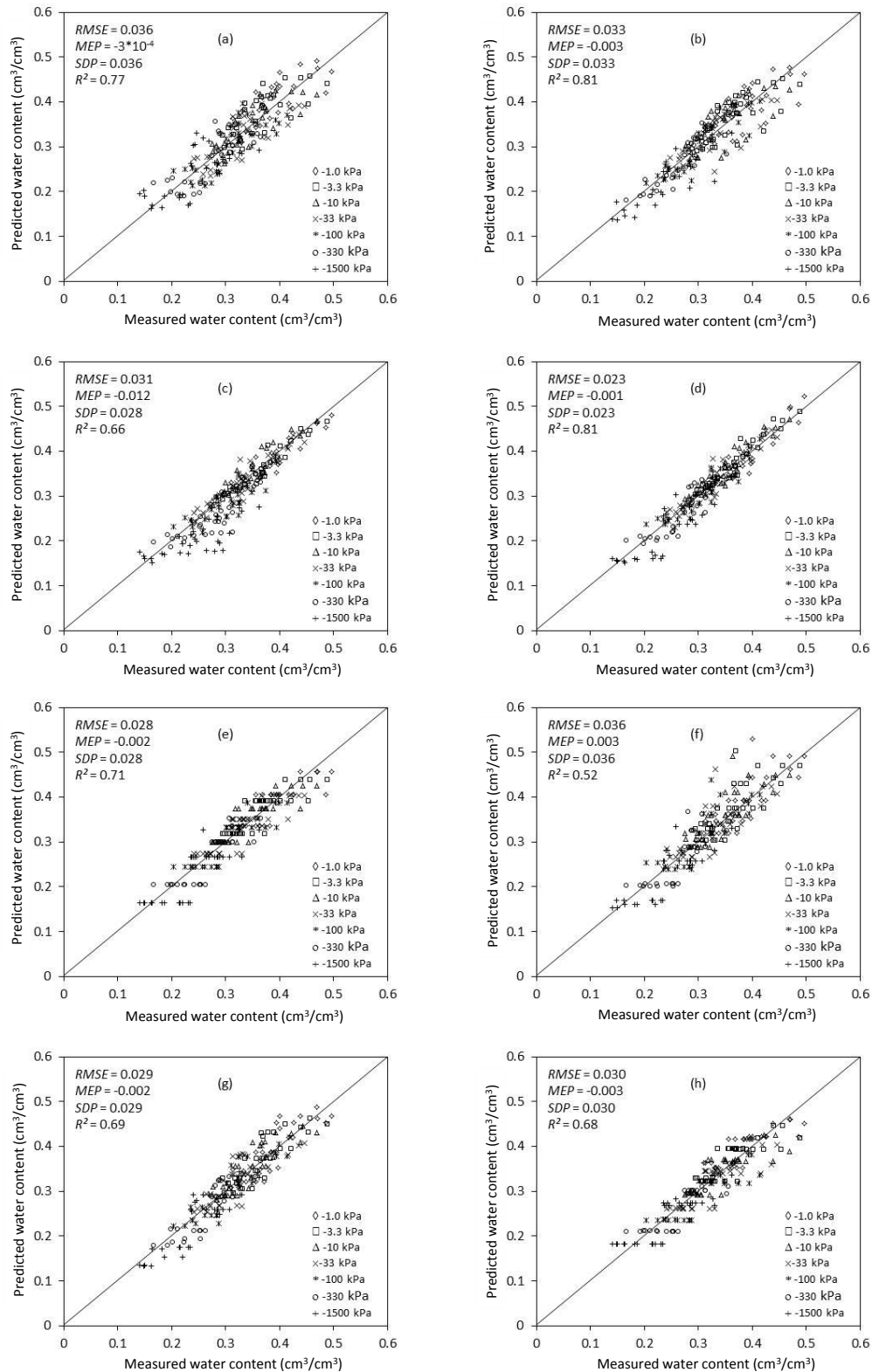
611  
612  
613  
614  
615  
616  
617



625 **Figure 2:** FAO triangle (FAO, 1990) of texture used (a), distribution of soil texture from samples used in this  
626 study to test the validity of the continuous- and class-PTFs selected, Syrian soil samples (b) and French soil  
627 samples (c).  
628  
629

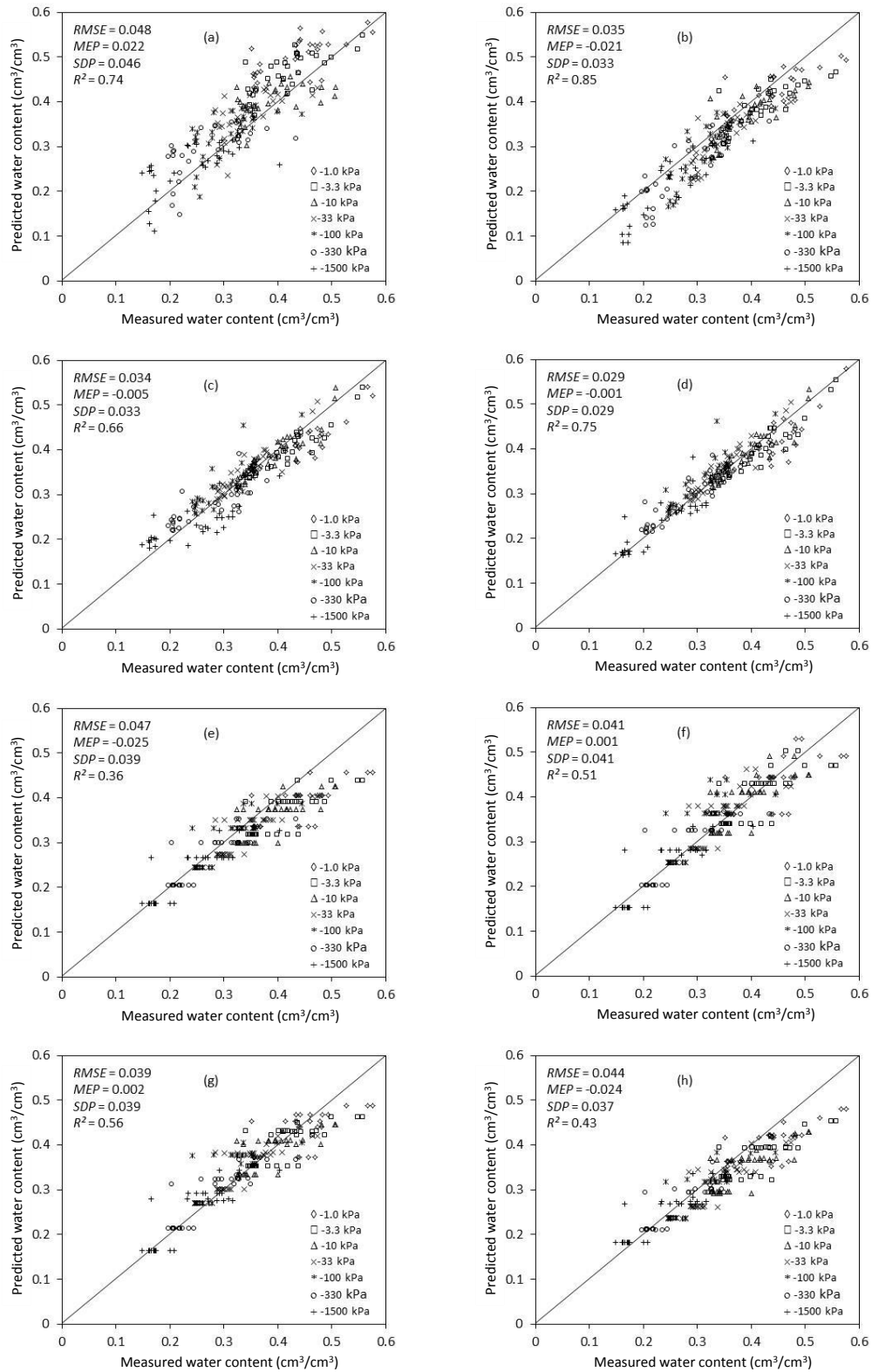
630  
631  
632  
633  
634  
635  
636





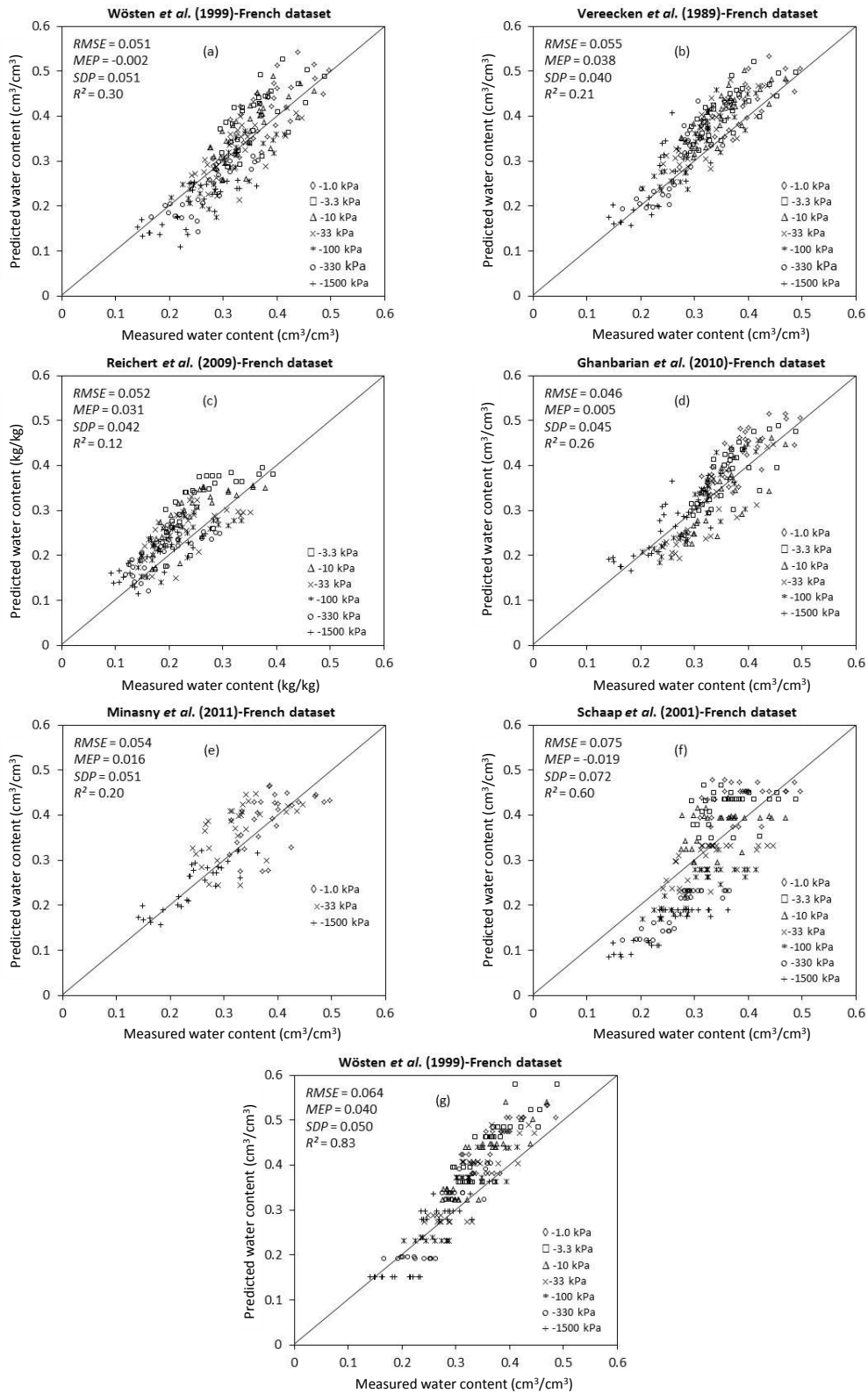
637  
638  
639  
640  
641  
642  
643  
644  
645  
646

**Figure 3:** Evaluation of the continuous-PTFs (a, b, c, d) and class-PTFs (e, f, g, h) developed with the French national database and applied to the French dataset. Continuous-PTFs developed for the parameters of the van Genuchten model (1980) (a), continuous-PTFs developed by multiple regression equations (b), continuous-PTFs with the volumetric water content at field capacity (c), class-PTFs with the volumetric water content at field capacity after stratification by class of texture (d), class-PFTs by class of texture (e), by class of texture and bulk density (f), by class of texture and bulk density after grouping according to the type of horizon (g) and finally by class of texture for the parameters of the van Genuchten model (1980) (h).



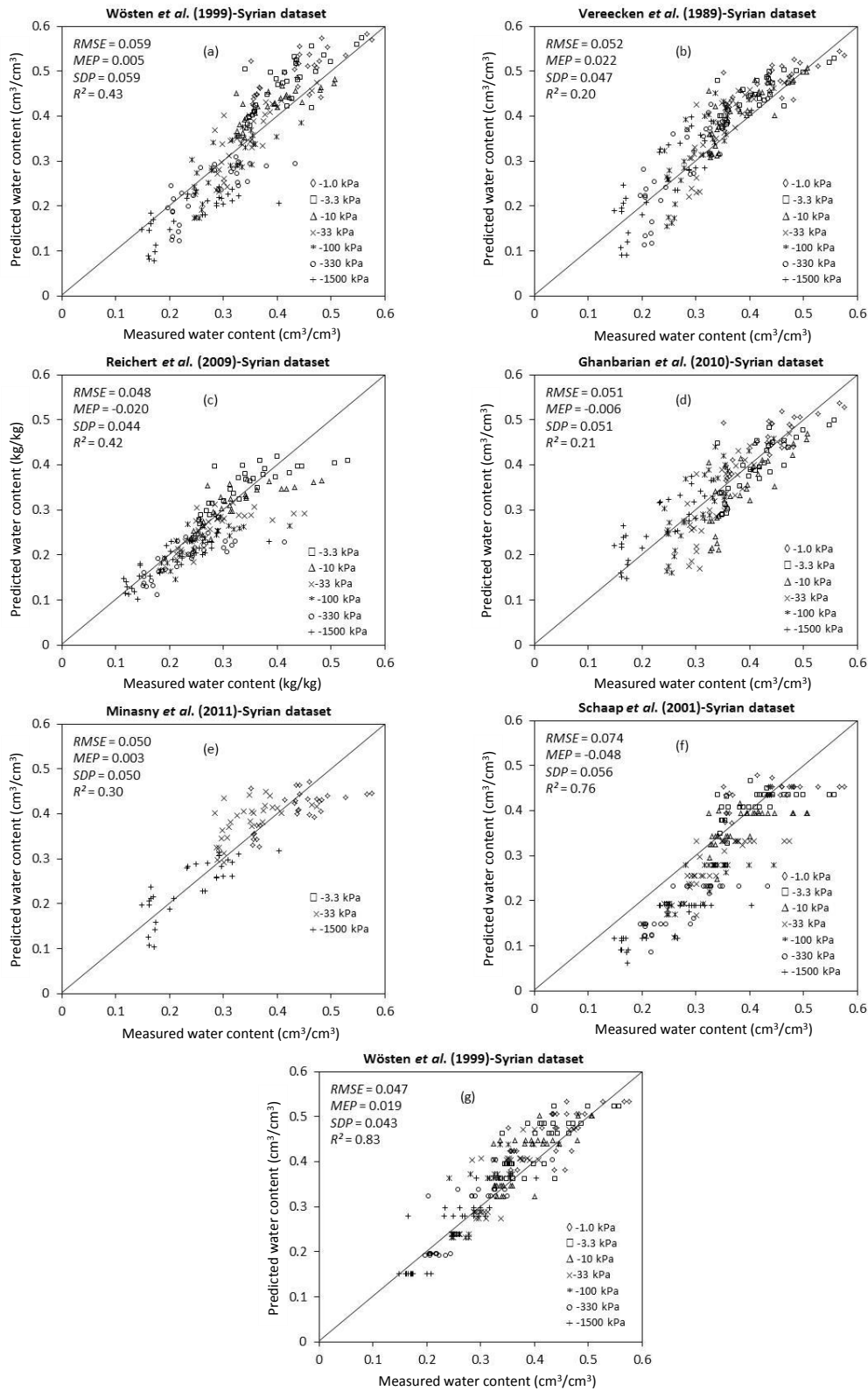
647  
648  
649  
650  
651  
652  
653  
654  
655  
656

**Figure 4:** Evaluation of the continuous-PTFs (a, b, c, d) and class-PTFs (e, f, g, h) developed with the French national database and applied to the Syrian dataset. Continuous-PTFs developed for the parameters of the van Genuchten model (1980) (a), continuous-PTFs developed by multiple regression equations (b), continuous-PTFs with the volumetric water content at field capacity (c), class-PTFs with the volumetric water content at field capacity after stratification by class of texture (d), class-PFTs by class of texture (e), by class of texture and bulk density (f), by class of texture and bulk density after grouping according to the type of horizon (g) and finally by class of texture for the parameters of the van Genuchten model (1980) (h).



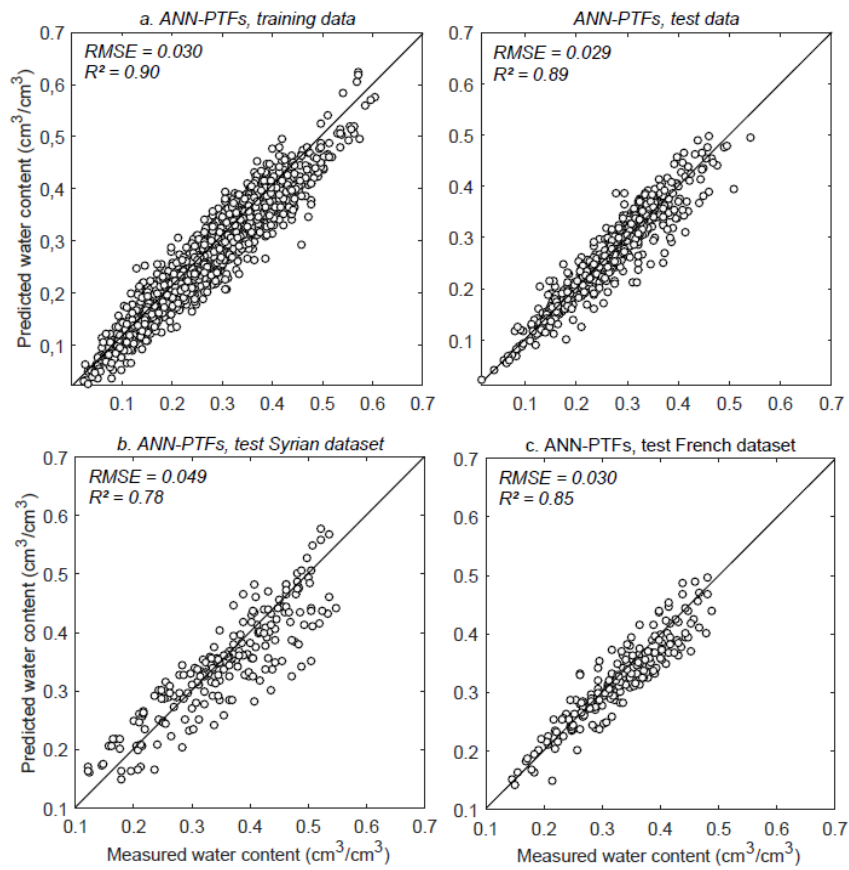
657  
658  
659  
660  
661  
662  
663  
664

**Figure 5:** Evaluation of the continuous-PTFs (a, b, c, d, e), and class-PTFs (f, g) selected in the literature when applied to the French dataset. R<sup>2</sup> were computed for all matric potential values together.



665  
 666  
 667  
 668  
 669

**Figure 6:** Evaluation of the continuous-PTFs (a, b, c, d, e), and class-PTFs (f, g) selected in the literature when applied to the Syrian dataset. R<sup>2</sup> were computed for all matric potential values together.



670  
671  
672  
673  
674

**Figure 7:** Measured and predicted water content (cm<sup>3</sup>/cm<sup>3</sup>) recorded with the artificial neural networks using soil properties (clay, silt, sand, organic carbon and bulk density) for the French national database (Al Majou *et al.*, 2008b) (a), Syrian dataset (b) and the French dataset (c).